

Novel insights into cyclooxygenases, linoleate diol synthases, and lipoxygenases from deuterium kinetic isotope effects and oxidation of substrate analogs

Inga Hoffmann^a, Mats Hamberg^b, Roland Lindh^c, Ernst H. Oliw^{a,*}

^a Division of Biochemical Pharmacology, Department of Pharmaceutical Biosciences, Uppsala University, Biomedical Center, SE-751 24 Uppsala, Sweden

^b Division of Physiological Chemistry II, Department of Medical Biochemistry and Biophysics, Karolinska Institutet, SE-171 77 Solna, Sweden

^c Department of Chemistry - Ångström, The Theoretical Chemistry Programme, Uppsala University, SE-751 20 Uppsala, Sweden

ARTICLE INFO

Article history:

Received 25 April 2012

Received in revised form 20 August 2012

Accepted 4 September 2012

Available online 12 September 2012

Keywords:

Animal heme peroxidase

Chiral phase HPLC

Fatty acid oxygenation

Kinetic isotope effect

Mass spectrometry

Oxygenation mechanism

ABSTRACT

Cyclooxygenases (COX) and 8R-dioxygenase (8R-DOX) activities of linoleate diol synthases (LDS) are homologous heme-dependent enzymes that oxygenate fatty acids by a tyrosyl radical-mediated hydrogen abstraction and antarafacial insertion of O₂. Soybean lipoxygenase-1 (sLOX-1) contains non-heme iron and oxidizes 18:2n-6 with a large deuterium kinetic isotope effect (D-KIE). The aim of the present work was to obtain further mechanistic insight into the action of these enzymes by using a series of n-6 and n-9 fatty acids and by analysis of D-KIE. COX-1 oxidized C₂₀ and C₁₈ fatty acids in the following order of rates: 20:2n-6 > 20:1n-6 > 20:3n-9 > 20:1n-9 and 18:3n-3 ≥ 18:2n-6 > 18:1n-6. 18:2n-6 and its geometrical isomer (9E,12Z)18:2 were both mainly oxygenated at C-9 by COX-1, but the 9Z,12E isomer was mostly oxygenated at C-13. A cis-configured double bond in the n-6 position therefore seems important for substrate positioning. 8R-DOX oxidized (9Z,12E)18:2 at C-8 in analogy with 18:2n-6, but the 9E,12Z isomer was mainly subject to hydrogen abstraction at C-11 and oxygen insertion at C-9 by 8R-DOX of 5,8-LDS. sLOX-1 and 13R-MnLOX oxidized [11S-²H]18:2n-6 with similar D-KIE (~53), which implies that the catalytic metals did not alter the D-KIE. Oxygenation of 18:2n-6 by COX-1 and COX-2 took place with a D-KIE of 3–5 as probed by incubations of [11,11-²H₂]- and [11S-²H]18:2n-6. In contrast, the more energetically demanding hydrogen abstractions of the allylic carbons of 20:1n-6 by COX-1 and 18:1n-9 by 8R-DOX were both accompanied by large D-KIE (>20).

© 2012 Elsevier B.V. All rights reserved.

1. Introduction

Polyunsaturated fatty acids can be oxygenated to important biological mediators. The first steps are usually catalyzed by fatty acid dioxygenases (DOX), which include heme-dependent DOX and lipoxygenases (LOX), or by monooxygenases (cytochromes P450) [1–4]. DOX contain heme and LOX non-heme iron (or rarely manganese). The DOX prototype is prostaglandin H (PGH) synthase-1, often designated cyclooxygenase (COX-1), and the most thoroughly studied LOX are soybean LOX-1 (sLOX-1), and human 5-LOX. In humans, COX and 5-LOX oxidize 20:4n-6 to prostaglandins and leukotrienes, respectively, which can activate G-protein coupled receptors in control of physiological functions, fever, inflammation, and development of cancer [3,4]. The versatile

function of eicosanoids has inspired the development of enzyme inhibitors and receptor agonists and antagonists [3,4]. In plants and fungi, the products of fatty acid DOX pathways, often referred to as oxylipins, participate in plant defence and fungal development and pathogenicity [2,5–7]. These oxylipins are formed by LOX or by heme-dependent DOX, viz., α-DOX of plants, and linoleate diol synthases (LDS) and related enzymes of fungi [2,6,8].

The LOX family constitutes homologous enzymes with a single peptide chain, folded into a small N-terminal β-barrel domain and a C-terminal domain with the catalytic metal [1,9]. All LOX contain catalytic iron except two enzymes with manganese [10,11]. The metal center redox cycles in a process of proton-coupled electron transfer from the C–H bond of a bis-allylic carbon to the catalytic base of the metal center (Fe³⁺+OH⁻), followed by antarafacial insertion of molecular oxygen [1]. The hydrogen abstraction is characterized by a large deuterium kinetic isotope effect (D-KIE) of ~80 [12]. Whether the D-KIE differs between Fe- and MnLOX is unknown. Differences in zero point energies and tunneling contribute to the D-KIE [13]. The zero point energy accounts for the 5- to 10-fold reduction of the reaction rate, which is due to the difference of activation energy needed for breaking C–H and C–D bonds (~1 kcal/mol). Larger D-KIE (>20) can be explained by hydrogen tunneling through the energy barrier, and this has been demonstrated for sLOX-1 by Klinman and co-workers [12,14]. The

Abbreviations: CP, chiral phase; COX, cyclooxygenase; DOX, dioxygenase; HODE, hydroxyoctadecadienoic acid; HETE, hydroxyeicosatetraenoic acid; HPOME, hydroperoxyeicosenoic acid; HPOME, hydroperoxyoctadecenoic acid; HEME, hydroxyeicosenoic acid; HOME, hydroxyoctadecenoic acid; D-KIE, deuterium kinetic isotope effect; LC, liquid chromatography; LDS, linoleate diol synthase; LOX, lipoxygenase; MS, mass spectrometry; NP, normal phase; [11R-²H] (9Z,12E)18:2, [11R-²H]-9Z,12E-octadecadienoic acid; PGH, prostaglandin H; RP, reversed phase; RSV, ram seminal vesicles; sLOX, soybean lipoxygenase; TIC, total ion current

* Corresponding author. Tel.: +46 18 471 44 55; fax: +46 184714847.

E-mail address: Ernst.Oliw@farmbio.uu.se (E.H. Oliw).

extent of tunneling during sLOX-1 catalysis is influenced by structural fluctuations and dynamic effects, as shown by these authors [14].

The heme-dependent DOX are homologous to animal heme peroxidases, and share fundamental catalytic properties [5,8,15]. Oxidation of the heme group of COX, α -DOX, and LDS generates in a peroxidase cycle a tyrosyl radical (Tyr \cdot), which catalyzes hydrogen removal. Tyr \cdot of COX-1 abstracts the *proS* hydrogen at C-13 of 20:4n–6, and this occurs with a D-KIE of ~2–3 at 20–30 °C [1,4,16], whereas Tyr \cdot of α -DOX abstracts hydrogen of palmitate with a D-KIE of ~54 [17]. A large D-KIE (>20) was also reported for COX-2 with perdeuterated 18:2n–6 as a substrate [18]. 7,8- And 5,8-LDS are fusion proteins of N-terminal domains with 8R-DOX activities and C-terminal P450 domains with diol synthase activities [19,20]. The Tyr \cdot of 8R-DOX of 7,8- and 5,8-LDS abstracts the *proS* hydrogen from the allylic position at C-8 of 18:2n–6 and 18:1n–9 [5,15,21], whereas the heme-thiolate abstracts the *proS* hydrogens at C-7 and C-5, respectively [5,21]. Recently, 5,8-LDS of *Aspergillus nidulans*¹ was found to catalyze these oxidations at C-8 and at C-5 of 18:1n–9 with D-KIE ~33 and ~1.1, respectively [22].

sLOX-1 and COX-1 oxidize 20:4n–6 with more than a 10-fold difference in D-KIE. This large difference is enigmatic, but could be due to kinetic factors, variable transitional complexes, and hydrogen donor–acceptor distances [16]. The C–H bond dissociation enthalpies of *bis*-allylic and allylic carbons are ~73 and ~87 kcal/mol, respectively [23], and this difference may influence the magnitude of the D-KIE. Suboptimal substrates may have higher D-KIE than native substrates due to steric factors.

The catalytic base of sLOX-1, Fe³⁺OH[–], is restricted to hydrogen abstraction from *bis*-allylic carbons [24], whereas Tyr \cdot of both COX-1 and LDS can oxidize allylic carbons [25]. Based on the large D-KIE of LOX, we hypothesized that a larger D-KIE of COX-1 and LDS might be observed during activation of C–H at singly allylic than *bis*-allylic positions since the contribution of hydrogen tunneling to the reaction rate is likely larger in reactions, which require more energy.

The first goal was to investigate mono- and polyunsaturated fatty acids and stereoisomers of 18:2n–6 as substrates of COX-1, 8R-DOX, and sLOX-1. The second goal was to determine the D-KIE during hydrogen abstraction and oxidation of *bis*-allylic carbons by COX-1 and COX-2, and allylic carbons by COX-1 and 8R-DOX. The third goal was to compare the D-KIE of LOX with Fe³⁺OH[–] and Mn³⁺OH[–] as catalytic bases.

2. Materials and methods

2.1. Materials

HPLC solvents (Lichrosolve) and routine chemicals were from Merck. 18:1n–9 (99%), 20:1n–6 (99%), 20:1n–9 (99%), 20:4n–6 (99%), and [¹³C₁₈]18:2n–6 were from Larodan. 18:1n–6 (99%), (9E,12Z)- and (9Z,12E)-18:2, 9R,5-HODE(10E,12E) and 9S-HODE(10E,12E) were from Lipidox. [11S-²H]18:2n–6 was prepared as described [5,26]. 20:3n–9 (99%) and purified ovine COX-2 (4.1 kU/mg) were from Cayman. 18:3n–6, 18:2n–6, (9E)-18:1, hematin, N-hydroxyphthalimide, ceric ammonium nitrate, lipoxidase type 5 (sLOX-1), and α -tocopherol were from Sigma-Aldrich. Fatty acids were dissolved in ethanol and stored in stock solutions (30–100 mM) at –20 °C. Photooxidation of [¹³C₁₈]18:2n–6 was performed with methylene blue in methanol. Microsomes of ram seminal vesicles (RSV) were prepared as described [27]. Recombinant 8R-DOX domains (5,8-LDS, residues 1–674 of *Aspergillus fumigatus*; 7,8-LDS, residues 1–673 of *Gaeumannomyces graminis*) were expressed in *Escherichia coli* [20], and referred to as 8R-DOX of 5,8- and 7,8-LDS. Full-length 5,8- and 7,8-LDS were expressed in *E. coli* [20]. Chiralcel OB-H (250 × 4.6 mm; Daicel) was purchased locally (Dalco Chromtech). Recombinant 13R-MnLOX was prepared as described [24].

2.2. Synthesis of mono- and dideuterated fatty acids

2.2.1. [11,11-²H₂]18:2n–6

2-Octynoic acid (9.2 g; Sigma-Aldrich) was refluxed for 1 h with 200 ml of methanol containing 2 ml conc. hydrochloric acid. The resulting methyl ester (8.9 g) was dissolved in 30 ml of diethyl ether and slowly added at 0 °C under magnetic stirring to a suspension of 1.8 g LiAlD₄ in 50 ml of diethyl ether. After stirring at 0 °C for 1 h, the reaction was quenched by slow addition of tetrahydrofuran/water and the alcohol (7.8 g) was isolated by extraction with diethyl ether. The material was dissolved in 50 ml of diethyl ether containing 1 ml of dry pyridine. PBr₃ (8.1 g) was slowly added at 0 °C under magnetic stirring, and the solution was subsequently refluxed for 1.5 h. [1,1-²H₂]1-bromo-2-octyne (7.9 g; yield, 63%) was obtained following purification on a silica gel column (elution with hexane). [1,1-²H₂]1-bromo-2-octyne (1.91 g) and methyl 9-decynoate (1.82 g) were stirred at 23 °C for 3 h with 1 eq. of CuI, 2 eq. of NaI, and 2 eq. of Cs₂CO₃, suspended in 30 ml of dry N,N-dimethylformamide (cf. [28]). After quenching with ammonium chloride, extraction with diethyl ether, drying over MgSO₄ and chromatography on silica gel, the methyl ester of the title compound was obtained in >90% yield. Part of this material (584 mg) was subjected to semihydrogenation using P-2 nickel [29] and purified by RP-HPLC. An aliquot of the deuterated methyl 9Z,12Z-octadecadienoate (184 mg) was saponified, and the free acid purified by RP-HPLC. This afforded the title compound (89 mg) as a colorless oil (purity >98%). The isotope composition as determined by GC-MS was 94.3% dideuterated, 5.1% monodeuterated, and 0.6% undeuterated molecules.

2.2.2. [8,8-²H₂]18:1n–9

8-Hydroxyoctanoic acid, prepared by alkali treatment of 8-bromooctanoic acid (Sigma-Aldrich), was treated with dihydropyran/*p*-toluenesulfonic acid to provide the tetrahydropyranyl ester/ether derivative. This material (5.99 g) in 100 ml of THF was refluxed with LiAlD₄ (3 g) for 2 h, and the deuterated 8-tetrahydropyranyloxy-1-octanol (4.47 g) was sequentially treated with methanesulfonyl chloride/triethylamine and sodium iodide to afford 8-tetrahydropyranyloxy-1-iodooctane (3.63 g; yield, 58%). An aliquot of this material (1 g; 2.9 mmol) in 5 ml of THF was added to the lithio derivative of 1-decyne (9 mmol) in 15 ml of THF and 5 ml of DMPU at 0 °C. The mixture was stirred at 0 °C for 2.5 h, quenched with ammonium chloride and extracted with diethyl ether. The resulting deuterated 1-tetrahydropyranyloxy-9-octadecyne was deprotected by treatment with *p*-toluenesulfonic acid, and the deuterated acetylenic alcohol (0.65 g; 2.43 mmol) was oxidized with pyridinium dichromate in N,N-dimethylformamide [30]. Semihydrogenation of the methyl ester using P-2 nickel [29], saponification, and purification by RP-HPLC afforded the title compound as a colorless oil (0.26 g; purity, >98%; >96% deuterated molecules; yield from the deuterated acetylenic alcohol, 38%).

2.2.3. [13,13-²H₂]20:1n–6

12-Bromo-1-dodecanol (1 g; Sigma-Aldrich) was treated with dihydropyran/*p*-toluenesulfonic acid to afford 1-bromo-12-tetrahydropyranyloxy-dodecane (1.3 g; yield, 99%). The Grignard derivative of this material (3.7 mmol) in 5 ml of THF was stirred at 23 °C for 5 min with 60 μ mol of dilithium tetrachlorocuprate(II) and then stirred for further 3 h following addition of 764 mg (4 mmol) of [1,1-²H₂]1-bromo-2-octyne. Extractive isolation with diethyl ether, removal of the tetrahydropyranyl blocking group by treatment with *p*-toluenesulfonic acid and chromatography on a silica gel column afforded material (0.54 g) consisting of the desired deuterated 14-eicosyn-1-ol admixed with a branched chain rearrangement product, ratio ~1:2. An aliquot of the mixture was oxidized by treatment with pyridinium dichromate in N,N-dimethylformamide [30], and pure deuterated 14-eicosynoic acid (70 mg) was obtained following RP-HPLC. Semihydrogenation of the methyl ester using P-2 nickel [29], saponification to the free acid, and

¹ 5,8-LDS is also designated psi producing oxygenase A (ppoA) [19].

purification by RP-HPLC afforded the title compound (45 mg; purity >98%; >96% deuterated molecules).

2.2.4. [11R-²H] (9Z,12E)-18:2

A recently described method was used [26]. Briefly, the epoxy alcohol methyl 11R,12R-epoxy-13S-hydroxy-9Z-octadecenoate (300 mg) was stirred with LiAlD₄ in diethyl ether affording trideuterated 12S,13S-dihydroxy-9Z-octadecenol. The *threo*-triol was sequentially converted into the title compound following monoacetylation of the primary alcohol function, conversion into the cyclic thionocarbonate derivative, stereospecific deoxygenation of the thionocarbonate, oxidation with pyridinium dichromate in *N,N*-dimethylformamide, and purification by RP-HPLC. The material obtained (purity >98%) was free from the 9Z,12Z-, 9E,12Z- and 9E,12E-octadecadienoate geometrical isomers as checked by GLC analysis of the methyl ester.

2.3. Autoxidation of 20:1n-6 and [13,13-²H₂]20:1n-6

5 mg 20:1n-6 and 0.2 mg α -tocopherol were treated with *N*-hydroxyphthalimide (0.8 eq.) and ceric ammonium nitrate (0.2 eq.) in acetonitrile (0.2 ml) under oxygen at 37 °C. [13,13-²H₂]20:1n-6 (5 mg) was oxidized in the same way. The reaction was followed by TLC and terminated by extractive isolation after 3–4 days, when >50% of 20:1n-6 was consumed. The products were separated by RP-HPLC (methanol/acetonitrile/water/acetic acid, 450/310/240/0.2) in three groups (13-HPEME, 16-HPEME, and mixture of 14- and 15-HPEME).

2.4. COX-1 activity assay by oxygen consumption

A YSI model 5300 biological oxygen monitor was used with a jacketed cell (1.5 ml; OX-15253, Gilson), an YSI 5331 oxygen probe, standard sensitivity membranes, and a magnetic stirrer. The cell was thermostated at 30 °C. Pre-warmed buffer (0.05 M Tris-HCl (pH 8.0 at 25 °C)/1 μ M hematin) at 30 °C and suspended microsomes of RSV on ice were added to the cell, and allowed to equilibrate for at least 2 min. The reaction was initiated by addition of fatty acids in ethanol through the stopper to a final concentration of 100 μ M and oxygen consumption was followed for a few minutes. The oxygen monitor was connected to an integrator (Hitachi-Merck D-2500). *K_m* of COX-1 and 20:1n-6 was estimated in triplicates by non-linear regression to the Michaelis–Menten equation with 10–300 μ M 20:1n-6 (GraFit software).

2.5. Enzyme assays by LC-MS and UV spectroscopy

2.5.1. COX-1

For structural analysis of products, microsomes of RSV were incubated with 100 μ M fatty acids in 0.1 M KHPO₄ buffer (pH 7.4)/2 mM EDTA for 30 min (37 °C). The reaction was stopped by addition of ethanol (4 vols.) and proteins were precipitated by centrifugation. The supernatant was evaporated to dryness and the products were then extracted (SepPak/C₁₈). Fatty acid hydroperoxides were reduced in some experiments to alcohols by treatment with triphenylphosphine or with NaBH₄.

2.5.2. 8R-DOX

Recombinant 8R-DOX of 5,8- and 7,8-LDS were incubated in 0.05 M Tris-HCl (pH 7.6)/5 mM EDTA/10% glycerol with 100 μ M (9E,12Z)18:2, (9Z,12E)18:2, and (9E)18:1 for 30 min on ice, and the products were extracted (SepPak/C₁₈) for LC-MS analysis.

2.5.3. sLOX-1

sLOX-1 (4–7 μ M) was incubated with 200 μ M (9E,12Z)18:2 or with 200 μ M [11R-²H] (9Z,12E)18:2 in 0.1 M NaBO₃ (pH 9.0; 23 °C), and the reaction was followed by UV analysis (235 nm) as described [24]. The products formed from 200 μ M (9E,12Z)18:2 were analyzed by chiral phase-HPLC (Reprosil Chiral AM) after addition of a small amount of 9- and 13-[¹³C₁₈]HODE.

2.6. Assays of non-competitive D-KIE

2.6.1. COX-1

We first compared the oxygen consumptions of COX-1 with 18:2n-6, [11S-²H]18:2, [11,11-²H₂]18:2n-6, 20:1n-6 and [13,13-²H₂]20:1n-6 as substrates. As the D-KIE of the latter was too large for quantification, we assayed the non-competitive D-KIE with LC-MS/MS. Microsomes of RSV (COX-1) were incubated in the same way as for analysis of oxygen consumption above (triplicate at 30 °C for 150 s) with 100 μ M 20:1n-6 and with 100 μ M [13,13-²H₂]20:1n-6. The reactions were ended by addition of methanol with the internal standard (0.3 μ g 13-HODE), hydroperoxides were reduced by NaBH₄, and the products were extracted as above and analyzed by LC-MS/MS (13-HODE, *m/z* 195; 13- and 15-HEME, *m/z* 225 and 227; [²H]13- and [²H]15-HEME, *m/z* 226 and 228).

2.6.2. COX-2

We compared the rate of oxidation of 100 μ M 18:2n-6, 100 μ M [11S-²H]18:2, and 100 μ M [11,11-²H₂]18:2n-6 by COX-2 (12 μ g) in triplicates in 0.5–1 ml 0.05 M Tris-HCl (pH 8.0)/5 mM EDTA/1 μ M hematin (30 °C; 3 min). The reactions were initiated by the addition of COX-2 and terminated by methanol. 13-HOTrE (125 ng) was added as an internal standard and hydroperoxides were reduced to alcohols by NaBH₄ in methanol (+4 °C). The main products, 9-HODE and [11R-²H]9-HODE (cf. [31]), respectively, were analyzed after extractive isolation as above by LC-MS/MS with monitoring of the internal standard (*m/z* 195) and *m/z* 171 from MS/MS analysis of *m/z* 295 and 296, respectively.

2.6.3. 8R-DOX

Recombinant 8R-DOX of 5,8- and 7,8-LDS were incubated with 100 μ M 18:1n-9 and [8,8-²H₂]18:1n-9 in triplicate on ice and the reactions were ended (after 1–3–10 min and 3–10–30 min, respectively) by addition of methanol with the internal standard (0.3 μ g 13-HODE). Hydroperoxides were reduced with NaBH₄ on ice, and the products were isolated on a cartridge of C₁₈ silica (SepPak/C₁₈). For LC-MS/MS, we monitored the internal standard at *m/z* 195, 8-HODE at *m/z* 157, and [²H]8-HODE at *m/z* 158.

2.6.4. sLOX-1 and 13R-MnLOX

The sLOX-1 and 13R-MnLOX activities were assayed in 0.1 M NaBO₃ buffer (pH 9.0; 23 °C) with UV analysis as described [24]. Dilutions of sLOX-1 and 13R-MnLOX were first titrated to oxidize 18:2n-6 at virtually the same rate, and we then compared the rates of oxidation of 100 μ M [11S-²H]18:2n-6.

2.7. HPLC and MS analyses

RP-HPLC-MS/MS analysis was performed on an octadecasilyl silica column (5 μ m, 100 Å, 150 × 2 mm; Phenomenex), which was eluted at 0.3 ml/min with methanol/water/acetic acid, 80/20/0.01. CP-HPLC-MS/MS analysis of hydroxyl fatty acids was performed on Chiralcel OB-H (250 × 4.6 mm), eluted at 0.5 ml/min with hexane/isopropyl alcohol/acetic acid, 95/5/0.01, or on Reprosil Chiral AM (250 × 2 mm), eluted at 0.2 ml/min with hexane/ethanol/acetic acid, 95/5/0.01. The effluents from the columns were combined with isopropyl alcohol/water (3/2) from a second HPLC pump and then introduced by electrospray into a linear ion trap mass spectrometer (LTQ, ThermoFisher). The transfer capillary was heated to 315 °C, the ion isolation width was set at 1.5 for anions of hydroxy fatty acids and 5 for anions of hydroperoxy fatty acids and 1.5 at the final selection of MS³ analysis. The collision energy was set at 1.7 V, and the ion tube lens at –110 to –130 V. We recorded five microscans and used the Gaussian algorithm for peak smoothing (Xcalibur software). Prostaglandin F_{1 α} was infused for tuning.

2.8. Steric analysis after ozonolysis

Steric analysis of HODE and HEME methyl esters was performed by derivatization into (–)-menthoxycarbonyl derivatives followed by GC–MS analysis of diastereomeric short chain fragments prepared by oxidative ozonolysis and methylation [32].

3. Results

3.1. Oxygenation of C_{18} and C_{20} fatty acids of the $n-6$ series by COX-1

$18:2n-6$ binds to the active site of COX-1 in analogy with $20:4n-6$ [33]. $18:2n-6$ was rapidly oxidized by COX-1 [34], and so was $18:3n-6$ (Fig. 1A). In analogy with $18:2n-6$, $18:3n-6$ was converted to 9-HOTrE as the main metabolite and to small amounts of 13-HOTrE (LC–MS/MS analysis; Fig. 2A). A minor polar metabolite yielded a MS/MS spectrum, which was identical to the MS/MS spectrum of dinor-PGE₁ (Fig. 2B), reported by Murphy et al. [35]. $18:1n-6$ was oxidized at a slower rate than $18:3n-6$ (Fig. 1A). Products formed from $18:1n-6$ were described previously (11-HOME(12Z) and 13-HOME(11E) in a ratio of ~4:1 [24]). Steric analysis by analysis of chiral fragments demonstrated optically pure 11S-HOME, ~93% 13S-HOME and ~7% 13R-HOME.

$20:1n-6$ was oxidized to a mixture of 13-HEME(14Z) and 15-HEME(13E) in a ratio of ~3:1 (Fig. 3A). Steric analysis showed that 13-HEME was formed with *S* configuration, and that 15-HEME consisted of ~93% of the *S* stereoisomer. The K_m was estimated to be $20 \pm 6 \mu\text{M}$. Racemic 13-HPHEME was not transformed to 15-HPHEME by COX-1,

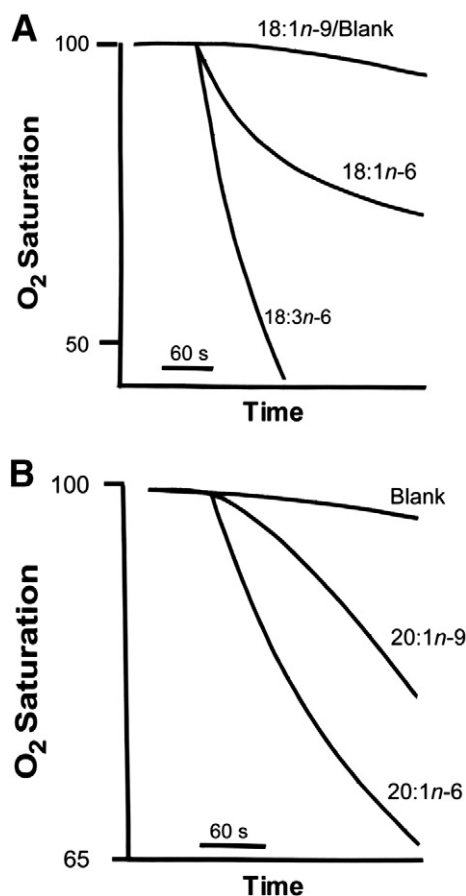


Fig. 1. Oxidation of $18:3n-6$, $18:1n-6$, and $20:1n-6$ by COX-1 monitored by an oxygen electrode. A, $18:1n-9$ was not a substrate, as the blank yielded an identical kinetic trace, whereas $18:1n-6$ was oxidized albeit at a slower rate than $18:3n-6$. B, $20:1n-6$ was oxidized in analogy with $18:1n-6$, but the kinetic trace of $20:1n-9$ differed as the rate increased in the course of 1–2 min.

indicating that the 13-peroxy radical may not be an intermediate in formation of 15-HPHEME.

3.2. Oxygenation of C_{18} and C_{20} fatty acids of the $n-9$ series by COX-1

$18:1n-9$ was not oxidized by COX-1 to a significant extent as judged from oxygen consumption assay (Fig. 1A), but $20:1n-9$ was oxidized, although slowly compared to $20:1n-6$ (Fig. 1B). The rate of oxidation of $20:1n-9$ increased gradually, and the rate of oxidation of Mead acid ($20:3n-9$) increased in a similar way.

From the initial rates of oxidation, the order of C_{20} fatty acids was $20:2n-6 > 20:1n-6 > 20:3n-9 > 20:1n-9$, and the order of C_{18} fatty acids was $18:3n-3 \geq 18:2n-6 > 18:1n-6$.

3.3. Oxygenation of (9E,12Z)- and (9Z,12E)18:2 by COX-1

(9E,12Z)18:2 was oxidized by COX-1 to 9-HODE and (9E,11E)13-HODE in a ratio of ~3:1. The absolute configuration was analyzed by CP-HPLC (Fig. 4A) and by ozonolysis. The latter analysis showed the following composition of regio- and stereoisomers: 9R (8%), 9S (76%), 13R (3%), and 13S (13%). These figures were in agreement with CP-HPLC analysis (Fig. 4A). 9S-HPODE can be visualized as formed by oxygen insertion at C-9 of the 1E,4Z-pentadiene radical with unchanged position of the side chain at C-9, as discussed below. For comparison, the proportions of products formed upon oxidation of $18:2n-6$ by COX-1 were 9R (73%), 9S (9%), 13R (1%), and 13S (17%) [34].

(9Z,12E)18:2 was oxidized to 13S-HPODE as the main metabolite. CP-HPLC of the products of (9Z,12E)18:2 is shown in Fig. 4B. Chemical degradation yielded 4 and 18% of the 9R and 9S stereoisomers, and 5 and 73% of the 13R and 13S stereoisomers. The mechanism of biosynthesis of 13S-HPODE was investigated with [$11R-^2\text{H}$] (9Z,12E)18:2. The latter was oxidized to 13S-HPODE with retention of the ^2H label, which also is the case during oxidation of $18:2n-6$. The oxidation at C-13 was therefore unlikely due to reverse orientation at the active site of COX-1. 13S-HPODE can be visualized as being formed from (9Z,12E)18:2 by oxygen insertion at C-13 of the 1Z,4Z-pentadiene radical, which is formed after rotation of the side chain at C-13 (cf. [1]).

3.4. Oxygenation of (9E,12Z)- and (9Z,12E)18:2 and (9E)18:1 by 8R-DOX

8R-DOX of 5,8-LDS, but not of 7,8-LDS, oxidized (9E,12Z)18:2. The products were separated by CP-HPLC and analyzed by MS/MS after reduction to alcohols as shown in Fig. 5. The main metabolite was 9R-HODE (>80%), but double bond isomers of 8- and 11-HODE were also detected. We conclude that (9E,12Z)18:2 was mainly subject to hydrogen abstraction at C-11 and oxygenation at C-9. Such oxygenation at C-9 could not be detected when $18:2n-6$ was the substrate.

As expected from oxidation of $18:1n-9$, the 8R-DOX of 7,8- and 5,8-LDS transformed (9Z,12E)18:2 to the 8-hydroperoxy metabolite as the main product (inset in Fig. 5). (9E)18:1 was oxidized at C-8 by 8R-DOX of 5,8-LDS but not by 7,8-LDS.

3.5. Oxygenation of (9Z,12E)18:2, [$11R-^2\text{H}$] (9Z,12E)18:2, and (9E,12Z)18:2 by sLOX-1

4 μM sLOX-1 (0.1 M NaBO₃; pH 9.0) oxidized 200 μM (9Z,12E)18:2 slowly to the 9-hydroperoxy metabolite with 10E,12E configuration as the main product (65%) and to 13-HPODE (35%; R/S ratio, 64/36). The UV absorbance at 235 nm increased linearly at a rate of ~0.03 AU/min. [$11R-^2\text{H}$] (9Z,12E)18:2 was not oxidized at a detectable rate under these conditions, suggesting inverse substrate orientation in comparison with $18:2n-6$ and a prominent D-KIE.

4 μM sLOX-1 oxidized (9E,12Z)18:2 more efficiently than (9Z,12E)18:2. After a prolonged kinetic lag time (2 min), the UV absorbance increased linearly at ~0.07 AU/min. CP-HPLC-MS/MS analysis showed

that 9-HPODE, in an R/S ratio of 60/40, was the main product (95%) along with the all *trans* isomer of 13-HPODE (5%). The R/S ratio of 9-HODE is in agreement with the report by Funk et al., but we could not detect significant formation of 13-HODE with 9Z,11E configuration [36].

3.6. D-KIE of COX, 8R-DOX, Mn-LOX, and sLOX-1

3.6.1. Oxidation of [11S-²H]- and [11,11-²H₂]18:2n-6 by COX-1

[11S-²H]18:2n-6 was oxidized at a slower rate than 18:2n-6 (Fig. 6A). The D-KIE averaged ~3.3, and this value appeared to be only slightly larger (~10%) for [11,11-²H₂]18:2n-6 as substrate. We conclude that [11S-²H]18:2n-6 is oxidized with a D-KIE in analogy with [13,13-²H₂]- and [13S-²H]20:4n-6 [16] (Table 1).

3.6.2. Oxidation of [13,13-²H₂]20:1n-6 by COX-1

20:1n-6 was oxidized by COX-1 as described above, but the rate of oxidation of [13,13-²H₂]20:1n-6 was insignificant in comparison with 20:1n-6, as judged by oxygen monitoring (Fig. 6B). Short time incubation (150 s, 30 °C) and LC-MS/MS analysis confirmed a D-KIE of this magnitude (~25), as illustrated in Fig. 7A. We conclude that allylic and *bis*-allylic carbons are oxidized by COX-1 with different D-KIE (Table 1).

3.6.3. Oxidation of [11S-²H]- and [11,11-²H₂]18:2n-6 by COX-2

The LC-MS/MS assay showed that [11S-²H]- and [11,11-²H₂]18:2n-6 were both oxidized at an average rate of 19% of 18:2n-6

(3 min, 30 °C), which suggested a D-KIE of ~5. Under these conditions, less than 5% of 18:2n-6 was oxidized.

3.6.4. Oxidation of [8,8-²H₂]18:1n-9 by 8R-DOX

The rates of oxidation of [8,8-²H₂]18:1n-9 and oleic acid by 8R-DOX of 7,8- and 5,8-LDS were determined by LC-MS/MS due to unstable readings with the oxygen electrode. The results from these LC-MS/MS analyses supported large D-KIE (>20), as illustrated by the measurements in Fig. 7B and C. This is in agreement with the D-KIE of 5,8-LDS of *A. nidulans* [22].

3.6.5. Oxidation of [11S-²H]18:2n-6 by 13R-MnLOX and sLOX-1

The relative D-KIE of the two LOX enzymes, measured by formation of 13-HPODE, differed by less than 10% (Fig. 7D). 13R-MnLOX also forms 15–20% 11S-HPODE lacking UV absorbance at 235 nm. The absolute D-KIE of this experiment (~53) was in the reported magnitude of the D-KIE of sLOX-1 [12].

3.7. D-KIE during autoxidation of [13,13-²H₂]20:1n-6

[13,13-²H₂]20:1n-6 was subject to autoxidation with N-hydroxyphthalimide, which generates a phthalimido-N-oxyl radical [37]. Analysis of the molecular anions of all the formed [13,13-²H₂]- and [13-²H]-labeled hydroperoxides (*m/z* 442 and 443) by LC-MS suggested a D-KIE of ~9, whereas MS³ analysis of [13-²H]15-HPEME and

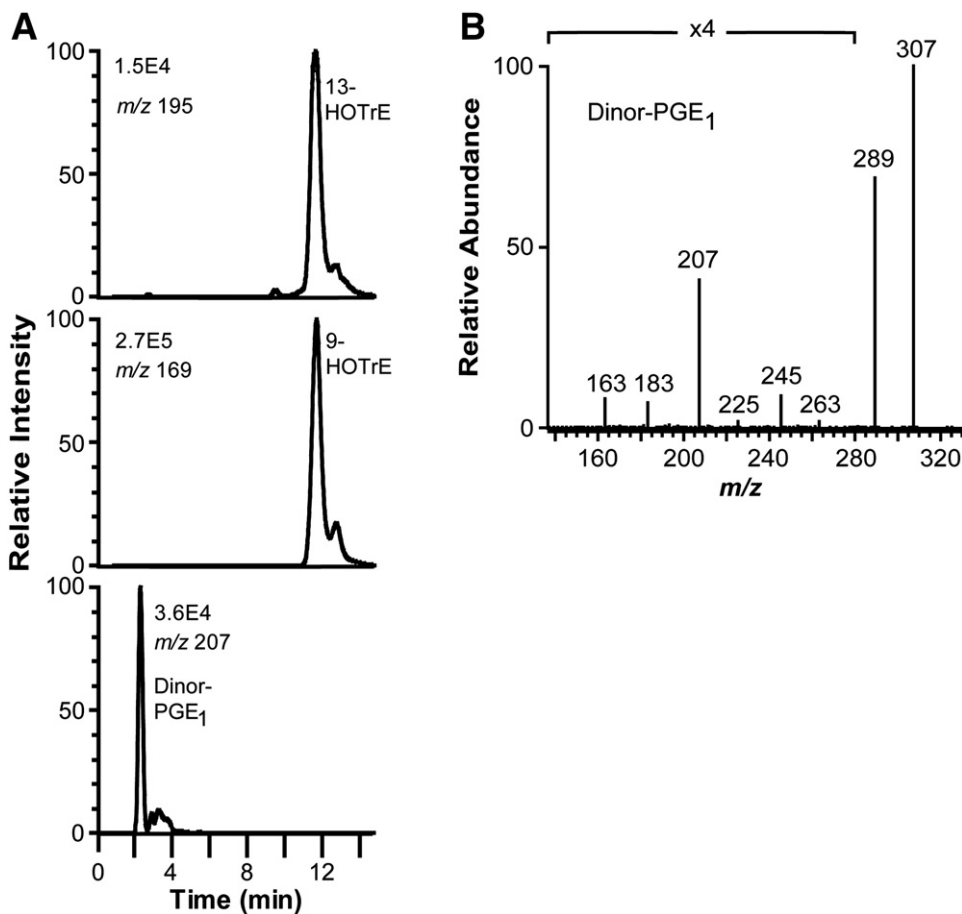


Fig. 2. The products formed from 18:3n-6 by COX-1 were analyzed by RP-HPLC-MS/MS. A, The top two chromatograms show intensities of selected ions specific for 13-HOTrE and 9-HOTrE, respectively, during MS/MS analysis (*m/z* 309 → full scan), and the latter was the main metabolite. The bottom chromatogram shows selective ion monitoring of *m/z* 207 during MS/MS analysis (*m/z* 325 → full scan). B, MS/MS spectrum of the polar metabolite was identical to the MS/MS spectrum of dinor-PGE₁, reported by Murphy and co-workers [35].

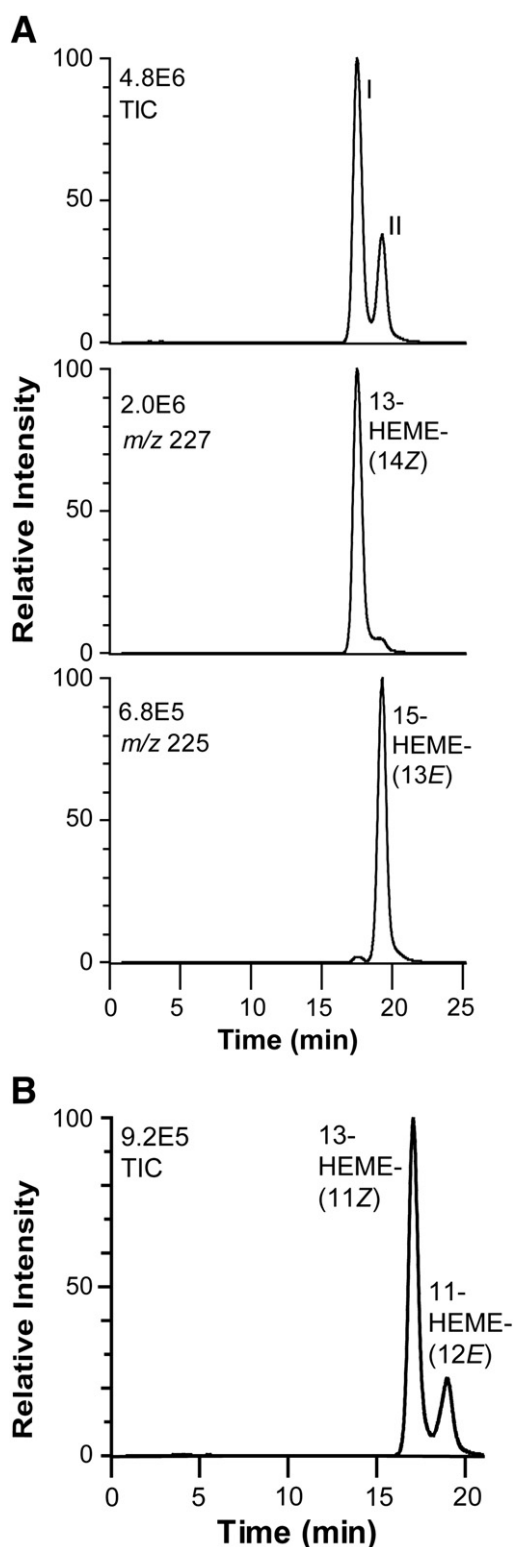


Fig. 3. RP-HPLC-MS/MS analysis of oxidation of 20:1n-6 and 20:1n-9 by COX-1. A, Analysis of products formed from 20:1n-6. The top chromatogram shows total ion current (TIC) during MS/MS analysis (m/z 325 \rightarrow full scan), whereas the two bottom chromatograms show intensities of selected ions specific for 13-HEME and 15-HEME, respectively. Peak I, 13-HEME, peak II, 15-HEME. B, The chromatogram shows TIC during MS/MS analysis (m/z 325 \rightarrow full scan) of products formed from 20:1n-9, and the main products were identified as marked (13- and 11-HEME).

[13,13- $^2\text{H}_2$]16-HPEME yielded a KIE of ~ 6 . For comparison, the D-KIE was 5.2–6.8 during autoxidation of [11,11- $^2\text{H}_2$]18:2 with the cumylperoxyl radical [38].

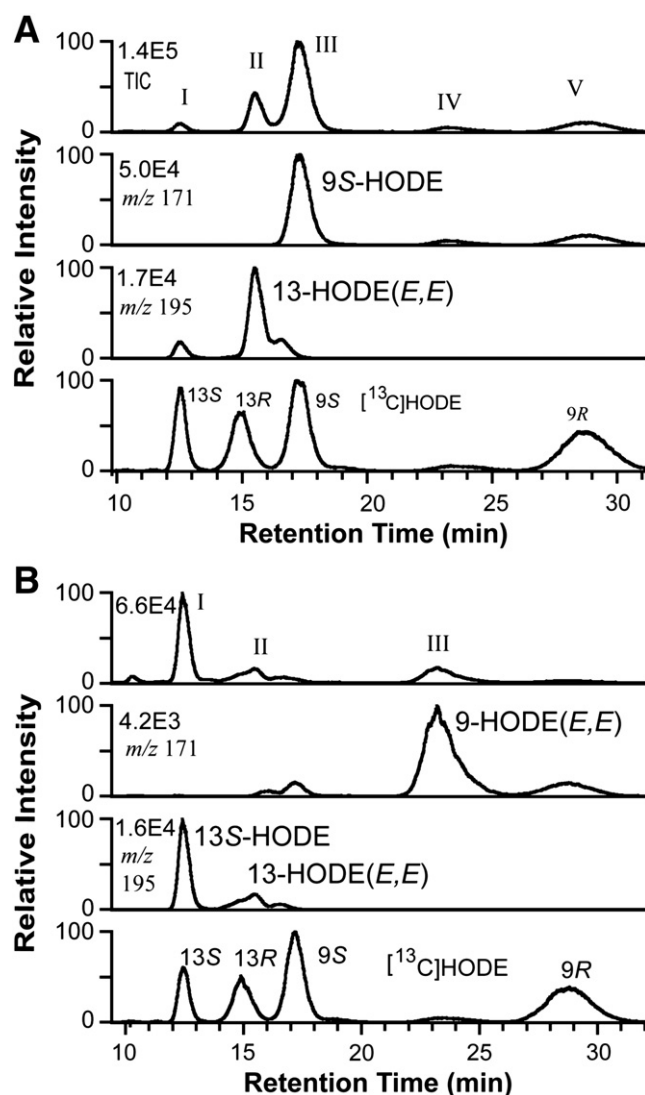


Fig. 4. LC-MS analysis of the oxidation of (9E,12Z)18:2 and (9Z,12E)18:2 by COX-1. A, CP-HPLC-MS/MS with separation of stereoisomers formed from (9E,12Z)18:2. Small amounts of 9- and 13- $^{13}\text{C}_{18}$]HODE were added to facilitate identification of stereoisomers (peak I, 13S-HODE, peak III, 9S-HODE, peak V, 9R-HODE, peak IV, 9-HODE(10E,12E), and peak II 13-HODE(9E,11E)). B, CP-HPLC-MS/MS with separation of stereoisomers formed from (9Z,12E)18:2, which were identified by aid of added $^{13}\text{C}_{18}$]HODE (peak I, 13S-HODE, peak II, 13R-HODE, and peak III, *trans-trans* 9-HODE). Separation on Chiralcel OB-H.

4. Discussion

We have investigated the reaction mechanisms of COX-1, COX-2, 8R-DOX, and lipoxygenases with selectively deuterated fatty acids. Oxidation of *cis-trans* isomers of 18:2n-6 and a selection of mono- and polyunsaturated fatty acids was also investigated. The reaction mechanisms of these enzymes are summarized in Figs. 8–10, and D-KIE in Table 1.

4.1. Influences of *cis-trans* isomers of 18:2n-6 and the n-6 double bond on catalysis

18:2n-6 is oxidized by COX-1 and COX-2 mainly to 9R-HPODE and to small amounts of 13S-HPODE. (9E,12Z)18:2 was oxidized by COX-1 to 9S-HPODE as the main metabolite. As expected, the 9E double bond thus changed the configuration of 9-HPODE from 9R to 9S, and this is in agreement with antarafacial hydrogen abstraction and oxygen insertion.

Unexpectedly, (9Z,12E)18:2 was mainly transformed to the S stereoisomer of 13-HPODE and not to the R stereoisomer (Fig. 8). Further

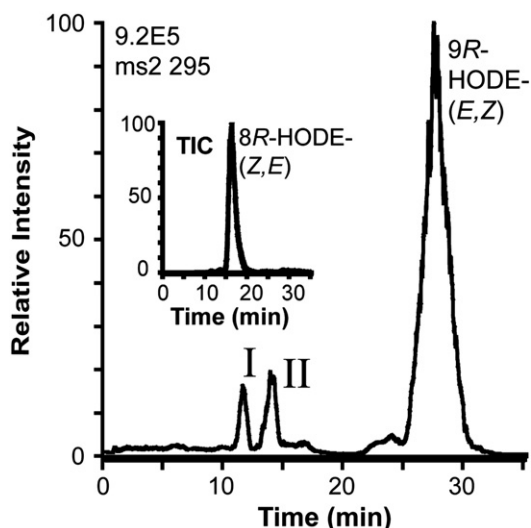


Fig. 5. Oxidation of (9*E*,12*Z*)18:2 and (9*Z*,12*E*)18:2 by 8*R*-DOX of 5,8-LDS. A, CP-HPLC-MS/MS analysis of products formed from (9*E*,12*Z*)18:2 after reduction to alcohols. The main product was identified as 9*R*-HODE, whereas MS/MS analysis of peaks I and II was consistent with 11-HODE and 8-HODE, respectively, presumably with (9*E*,12*Z*) configuration. The inset shows CP-HPLC-MS/MS analysis of products formed from (9*Z*,12*E*)18:2 after reduction to alcohols; the main product was 8-HODE, likely with 9*Z*,12*E* configuration. Analysis on Chiralcel OB-H.

analysis with (9*Z*,12*E*)[11*R*-²H]18:2 showed that this was not due to reverse orientation in the active site, as the ²H-label was retained in 13*S*-HPODE. An antarafacial oxygenation mechanism could be explained, as outlined in Fig. 8, by bond rotation at C-13 with formation of the 1*Z*,4*Z*-pentadiene radical, as previously described in sLOX-1 catalysis [36]. The effects of bond rotation on radical conformation and the configuration of oxygen insertion by COX and LOX were recently reviewed by Schneider and co-workers [1].

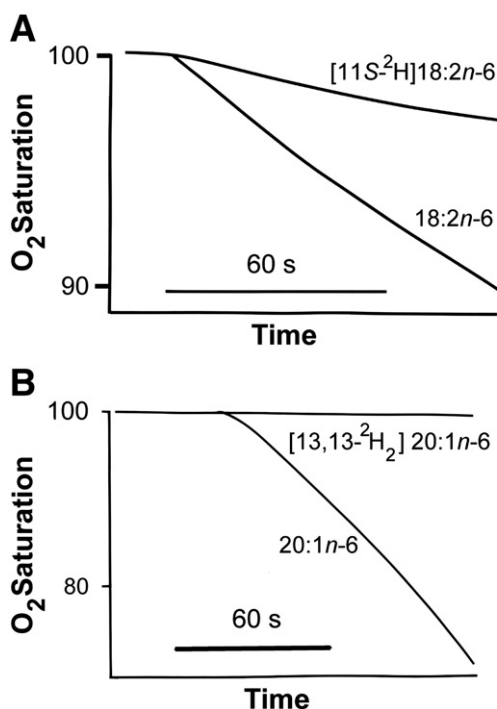


Fig. 6. Oxidation of deuterated fatty acids by COX-1 with monitoring of oxygen consumption. A, Oxidation of 18:2*n*–6 and [11*S*-²H]18:2*n*–6. B, Oxidation of 20:1*n*–6 and [13,13-²H₂]20:1*n*–6.

8*R*-DOX of *A. fumigatus* oxidized (9*Z*,12*E*)18:2 in analogy with 18:1*n*–9, but (9*E*,12*Z*)18:2 was transformed to 9*R*-HPODE as the main metabolite by 8*R*-DOX of 5,8-LDS. This occurred apparently by *bis*-allylic hydrogen abstraction (Fig. 9), but the relation of hydrogen abstraction to oxygen insertion was not further investigated. Small amounts of products formed by hydrogen abstraction and oxidation at C-8 and C-11 were also formed.

COX-1 oxidized 20:1*n*–6 by hydrogen abstraction at C-13, which was followed by oxygen insertion at C-13 and, after double bond migration, at C-15 (Fig. 8); it is noteworthy that the *proR* hydrogen at C-13 of 20:1*n*–6 will be designated *proS* at C-13 of 20:4*n*–6 due to the Cahn–Ingold–Prelog nomenclature. These products, 13- and 15-HPEME, were formed with high stereospecificity (>93% *S* configuration). 18:1*n*–6 was oxidized in the same way. The *n*–6 double bond and chain length seemed to be important, as 18:1*n*–9 was not oxidized by COX-1 and 20:1*n*–9 and 20:3*n*–9 were oxidized only slowly compared to 20:1*n*–6 and 20:2*n*–6.

It is well known that COX-1 accepts chain elongation of 20:4*n*–6 to adrenic acid (22:4*n*–6), which is transformed to dihomopGE₂ [39]. Chain shortening is also accepted, as COX-1 transformed 18:3*n*–6 to dinor-PGE₁ although only a small fraction of the peroxy radical of 9*R*-HPOTrE(*n*–6) was converted in this way.

The tertiary structure and catalytic domains of COX-1 and myeloperoxidase have been described as strikingly similar [40]. It is therefore of interest that COX-1 abstracts the *proR* hydrogen of 20:1*n*–6 (Fig. 8), whereas 8*R*-DOX abstracts the *proS* hydrogen of 18:1*n*–9 (Fig. 9). This observation suggests that 8*R*-DOX could bind fatty acids in opposite head-tail orientation than COX-1.

sLOX-1 abstracts the *proS* hydrogen at C-11 of 18:2*n*–6 and forms 13*S*-HPODE as the main metabolite at pH 9 (Fig. 10). At a lower pH with uncharged carboxyl group, 18:2*n*–6 binds in the opposite orientation with biosynthesis of 9*S*-HPODE [41]. sLOX-1 was reported by Funk et al. [36] to oxidize the two *cis*-*trans* isomers of 18:2*n*–6 at neutral pH. To ascertain the importance of the charged carboxyl group we re-investigated these oxidations at pH 9.

(9*Z*,12*E*)18:2 was oxidized slowly to the *trans* isomer of 9-HODE and to 13*R*-HPODE as the two main products (Fig. 10), essentially as reported previously [36]. [11*R*-²H] (9*Z*,12*E*)18:2 was not oxidized at a detectable rate, which implies that (9*Z*,12*E*)18:2 likely binds to the active site of sLOX-1 in reverse orientation and presents the *proR* hydrogen at C-11 for abstraction. 13*R*-HPODE might be formed by bond rotation at C-13, as outlined in Fig. 10.

(9*E*,12*Z*)18:2 was mainly oxidized at C-9 (>95%) to 9-HPODE in an *R/S* ratio of 60/40. 13-HODE was formed with 9*E*,11*E* configuration. We could not find significant biosynthesis of 13-HODE having a 9*Z* double bond; this differs from results of bond rotation at C-9/C-10 with formation of 13-HODE with 9*Z* configuration observed at neutral pH [36]. The observation that 9-HPODE was almost racemic suggested that this fatty acid may partly bind the active site in opposite orientations for hydrogen abstraction and oxygenation (Fig. 10).

4.2. D-KIE of lipoxygenases, cyclooxygenases, and 8*R*-DOX

Labeling of fatty acids with tritium or deuterium has been instrumental for analysis of reaction mechanisms of fatty acid oxygenases [42]. This

Table 1
Summary of apparent D-KIE of dioxygenase reactions.

Enzymes	Hydrogen abstraction at <i>bis</i> -allylic carbons	Allylic carbons
COX-1	~3	~25
COX-2	~5	ND
8 <i>R</i> -DOX	ND	>20
sLOX-1	~53	–
MnLOX	~53	–

ND, not determined. –, oxidized at insignificant rates compared to *bis*-allylic carbons.

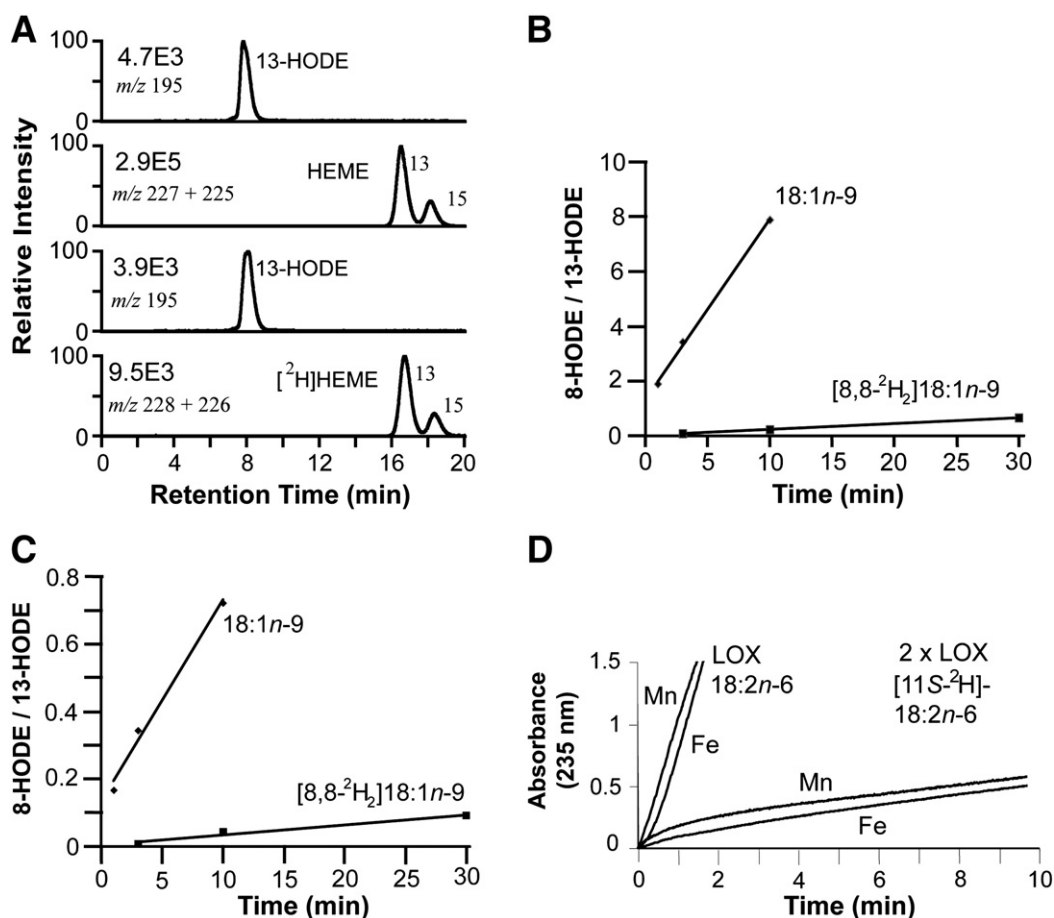


Fig. 7. LC-MS/MS analysis of apparent D-KIE of COX-1 and 8R-DOX and UV analysis of relative D-KIE of 13R-MnLOX and sLOX-1. A, LC-MS analysis of the oxidation of 20:1n-6 and [13,13-²H₂]20:1n-6 by COX-1 with aid of an internal standard (13-HODE). The first and second chromatograms show the signal intensities of the internal standard and 13- and 15-HEME. The third and fourth chromatograms show the signal intensities of the internal standard and deuterated 13- and 15-HEME. The signal intensities suggest a D-KIE of ~25, and the illustrated chromatograms are median values of triplicate analysis (30 °C, 150 s). B, Oxidation of 18:1n-9 and [8,8-²H₂]18:1n-9 by 8R-DOX of 7,8-LDS (mean of triplicate analysis; +4 °C) at different time points assessed with an internal standard (13-HODE). C, Oxidation of 18:1n-9 and [8,8-²H₂]18:1n-9 by 8R-DOX of 5,8-LDS. D, UV analysis of products formed from 18:2n-6 and [11S-²H]18:2n-6 by 13R-MnLOX and sLOX-1. The latter was incubated with double enzyme concentration.

led to the discovery of the prominent D-KIE of sLOX-1 [12,43]. The D-KIE of 13R-MnLOX and sLOX-1 appeared to be rather similar (Fig. 7D). We conclude that the two different catalytic metals may not alter the D-KIE under our experimental conditions (23 °C, pH 9.0) although the redox potentials of the free metals, Mn³⁺/Mn²⁺ and Fe³⁺/Fe²⁺, differ by a factor of 2 [24].

We found that COX-1 oxidized the allylic C-13 of 20:1n-6 with at least a 7-fold larger D-KIE than the *bis*-allylic C-11 of 18:2n-6 under identical experimental conditions. These results suggest that D-KIE differ between allylic and *bis*-allylic hydrogen abstraction. The contribution of tunneling to D-KIE could be influenced by the energy necessary for hydrogen abstraction, the surface potential of the enzyme, and by kinetic factors. Kulmacz and co-workers investigated the oxidation of [13S-²H]- and [13,13-²H₂]20:4n-6 by purified COX-1 at different experimental conditions, and reported a weakly temperature-dependent D-KIE of 2–3 [16]. In contrast, it was shown that D-KIE of recombinant COX-2 with [²H₃₁]18:2n-6 as substrate varied with the experimental conditions [18], but that it was larger than reported for 20:4n-6 [16]. These results may appear contradictory, but the perdeuterated [²H₃₁]18:2n-6 may conceivably interact with the surface of the active site of COX in a less beneficial manner for catalysis than [13S-²H]20:4n-6, [11S-²H]18:2n-6, and [11,11-²H₂]18:2n-6. We found that the latter two were oxidized by COX-1 and COX-2 with apparent D-KIE of 3–5. Remote deuterium atoms may exert secondary effects, as [5,5-²H₂]18:1n-9 was oxidized at C-8 by 5,8-LDS of *A. nidulans*¹ at a lower rate than 18:1n-9 [22].

In analogy with the allylic oxidation of 20:1n-6 by COX-1, 8R-DOX of 7,8- and 5,8-LDS oxidized the allylic C-8 of 18:1n-9 with a large D-KIE. This is also in agreement with a recent report on 5,8-LDS of *A. nidulans*¹ [22]. The D-KIE of COX during oxidation of an allylic position can be compared to the D-KIE during oxidation at C-2 of [2,2-²H₂]16:0 by α-DOX, which also requires more energy than oxidation of *bis*-allylic carbons. D-KIE of α-DOX averaged 31 at pH 7.2 [17]. The large apparent D-KIE of COX-1, 8R-DOX, and α-DOX of at least 20 suggest a significant contribution of hydrogen tunneling to these reactions. The midpoint redox potential of Tyr•/Tyr is 0.94 V (pH 7.0; 25 °C) [44], which is apparently sufficient for oxidation of both allylic and *bis*-allylic carbons, whereas the redox potential of sLOX-1 has been estimated to be ~0.6 V [45]. In addition, hydrogen donor and acceptor distances and the reversibility of hydrogen transfer may conceivably differ between COX and LOX.

5. Conclusion

COX-1 binds mono- and polyunsaturated fatty acids with the omega end first. The *cis* n-6 double bond facilitated allylic oxidation by COX-1 in comparison with *cis* n-9 fatty acids. *bis*-Allylic oxidation by COX-1 was catalyzed more efficiently and with insignificant hydrogen tunneling compared to allylic oxidation. COX-1 oxidized (9Z,12E)18:2 with bond rotation at C-13, whereas 8R-DOX shifted hydrogen abstraction of (9E,12Z)18:2 to C-11 and oxygen insertion to C-9. Fe or Mn as catalytic metal of LOX appeared to have little influence on D-KIE.

COX-1

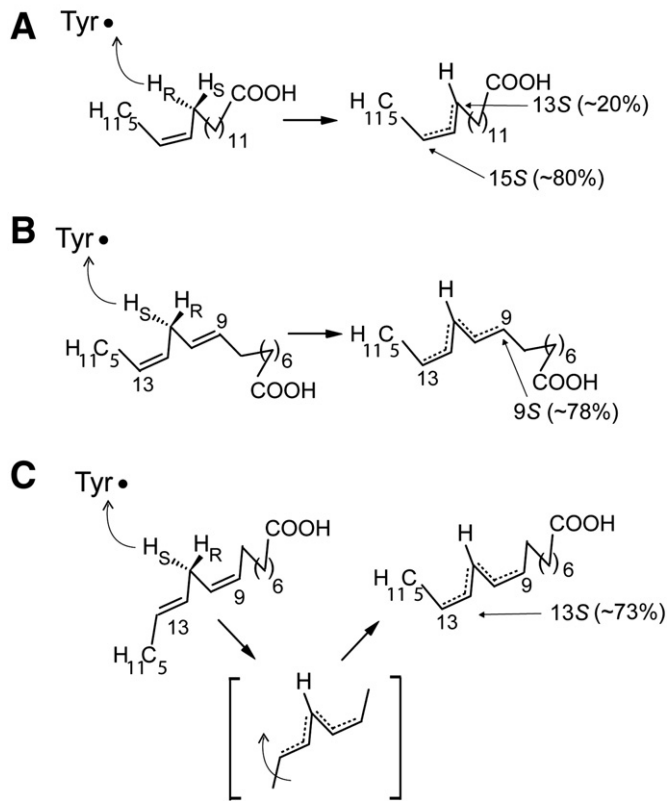


Fig. 8. Overview of hydrogen abstraction and formation of major oxidation products of 20:1n–6, (9E,12Z)18:2 and (9Z,12E)18:2 by COX-1. A, The *proR* hydrogen of C-13 is abstracted and oxygen is inserted at C-13 and at C-15. B, Oxidation of (9E,12Z)-18:2 to 9S-HPODE as the main metabolite. C, Oxidation of (9Z,12E)-18:2 to 13S-HPODE as the main metabolite. [11R-²H] (9Z,12E)-18:2 was oxidized with retention of the deuterium label, supporting unchanged orientation in the active site. 13S-HPODE could be formed by bond rotation at C-13 of the pentadienyl radical as indicated.

8R-DOX

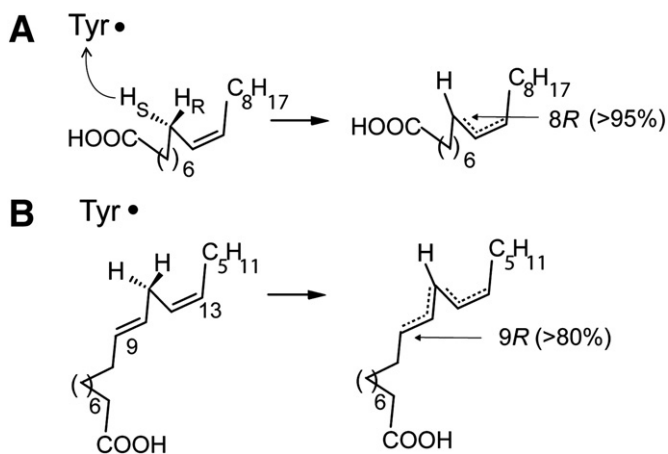


Fig. 9. Overview of formation of major oxidation products of 18:1n–9 and (9E,12Z)18:2 by 8R-DOX. A, Hydrogen abstraction and oxygenation at C-8 of 18:1n–9 occur in an antarafacial way [21]. B, (9E,12Z)18:2 is oxidized by hydrogen abstraction at C-11 and oxygen insertion at C-9 with formation of 9R-HPODE; the steric relation of hydrogen abstraction and oxygen insertion has not been determined.

sLOX-1

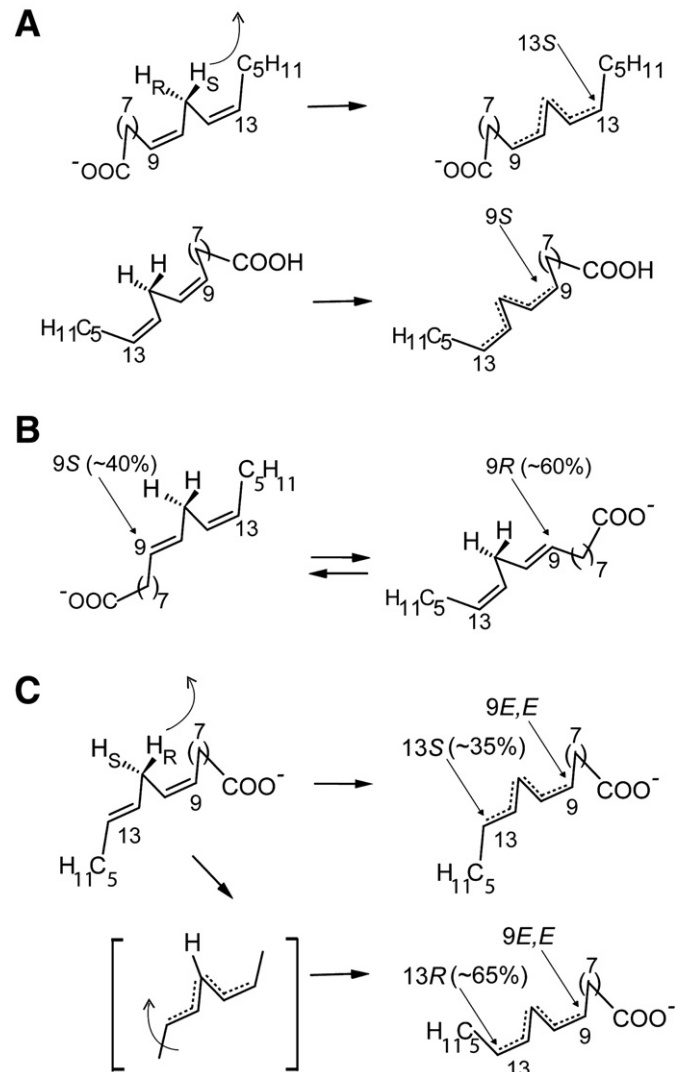


Fig. 10. Overview of hydrogen abstraction and formation of major oxidation products of 18:2n–6, (9E,12Z)18:2 and (9Z,12E)18:2 by sLOX-1. A, 18:2n–6 is oxidized at C-13 at alkaline pH (top) in normal orientation and at C-9 at acidic pH (bottom) to 9S-HPODE by inverse orientation in the active site. B and C, The two *cis-trans* fatty acids are mainly oxidized at the *trans* double bonds. (9Z,12E)18:2 in B appeared to be oxidized in both orientations as this fatty acid was oxidized to 9-HPODE in an *R/S* ratio of 60/40. (9E,12Z)18:2 in C was likely oxidized by abstraction of the *proS* hydrogen at C-11 in the reverse orientation, as [11R-²H](9E,12Z)18:2 was a poor substrate. 13R-HPODE might be formed by bond rotation at C-13 as indicated.

Acknowledgements

This work was supported by VR (03X-06523) and by the Knut and Alice Wallenberg Foundation (KAW 2004.0123).

References

- [1] C. Schneider, D.A. Pratt, N.A. Porter, A.R. Brash, Control of oxygenation in lipoxygenase and cyclooxygenase catalysis, *Chem. Biol.* 14 (2007) 473–488.
- [2] A. Andreou, I. Feussner, Lipoxygenases – structure and reaction mechanism, *Phytochemistry* 70 (2009) 1504–1510.
- [3] J.Z. Haeggström, C.D. Funk, Lipoxygenase and leukotriene pathways: biochemistry, biology, and roles in disease, *Chem. Rev.* 111 (2011) 5866–5898.
- [4] W.L. Smith, Y. Urade, P.J. Jakobsson, Enzymes of the cyclooxygenase pathways of prostanoid biosynthesis, *Chem. Rev.* 111 (2011) 5821–5865.

- [5] U. Garscha, F. Jermerén, D. Chung, N.P. Keller, M. Hamberg, E.H. Oliw, Identification of dioxygenases required for *Aspergillus* development. studies of products, stereochemistry, and the reaction mechanism, *J. Biol. Chem.* 282 (2007) 34707–34718.
- [6] F. Brodhun, I. Feussner, Oxylipins in fungi, *FEBS J.* 278 (2011) 1047–1063.
- [7] J. Vicente, T. Cascon, B. Vicedo, P. Garcia-Agustin, M. Hamberg, C. Castresana, Role of 9-lipoxygenase and alpha-dioxygenase oxylipin pathways as modulators of local and systemic defense, *Mol. Plant* 5 (2012) 914–928.
- [8] M. Hamberg, I. Ponce de Leon, M.J. Rodriguez, C. Castresana, Alpha-dioxygenases, *Biochem. Biophys. Res. Commun.* 338 (2005) 169–174.
- [9] I. Ivanov, D. Heydeck, K. Hofheinz, J. Roffeis, V.B. O'Donnell, H. Kuhn, M. Walther, Molecular enzymology of lipoxygenases, *Arch. Biochem. Biophys.* 503 (2010) 161–174.
- [10] C. Su, E.H. Oliw, Manganese lipoxygenase. Purification and characterization, *J. Biol. Chem.* 273 (1998) 13072–13079.
- [11] A. Wennman, F. Jermerén, M. Hamberg, E.H. Oliw, Catalytic convergence of Mn- and iron lipoxygenases by replacement of a single amino acid, *J. Biol. Chem.* 287 (2012) 31757–31765.
- [12] M.J. Knapp, J.P. Klinman, Environmentally coupled hydrogen tunneling. Linking catalysis to dynamics, *Eur. J. Biochem.* 269 (2002) 3113–3121.
- [13] F.H. Westheimer, The magnitude of the primary kinetic isotope effect for compounds of hydrogen and deuterium, *Chem. Rev.* 61 (1961) 265–273.
- [14] M.P. Meyer, D.R. Tomchick, J.P. Klinman, Enzyme structure and dynamics affect hydrogen tunneling: the impact of a remote side chain (I553) in soybean lipoxygenase-1, *Proc. Natl. Acad. Sci. U. S. A.* 105 (2008) 1146–1151.
- [15] C. Su, M. Sahlin, E.H. Oliw, A protein radical and ferryl intermediates are generated by linoleate diol synthase, a ferric heme protein with dioxygenase and hydroperoxide isomerase activities, *J. Biol. Chem.* 273 (1998) 20744–20751.
- [16] G. Wu, J.M. Lu, W.A. van der Donk, R.J. Kulmacz, A.L. Tsai, Cyclooxygenase reaction mechanism of prostaglandin H synthase from deuterium kinetic isotope effects, *J. Inorg. Biochem.* 105 (2011) 382–390.
- [17] A. Gupta, A. Mukherjee, K. Matsui, J.P. Roth, Evidence for protein radical-mediated nuclear tunneling in fatty acid alpha-oxygenase, *J. Am. Chem. Soc.* 130 (2008) 11274–11275.
- [18] H.H. Danish, I.S. Doncheva, J.P. Roth, Hydrogen tunneling steps in cyclooxygenase-2 catalysis, *J. Am. Chem. Soc.* 133 (2011) 15846–15849.
- [19] F. Brodhun, C. Göbel, E. Hornung, I. Feussner, Identification of PpoA from *Aspergillus nidulans* as a fusion protein of a fatty acid heme dioxygenase/peroxidase and a cytochrome P450, *J. Biol. Chem.* 284 (2009) 11792–11805.
- [20] I. Hoffmann, F. Jermerén, U. Garscha, E.H. Oliw, Expression of 5,8-LDS of *Aspergillus fumigatus* and its dioxygenase domain. A comparison with 7,8-LDS, 10-dioxygenase, and cyclooxygenase, *Arch. Biochem. Biophys.* 506 (2011) 216–222.
- [21] M. Hamberg, L.Y. Zhang, I.D. Brodowsky, E.H. Oliw, Sequential oxygenation of linoleic acid in the fungus *Gaeumannomyces graminis*: stereochemistry of dioxygenase and hydroperoxide isomerase reactions, *Arch. Biochem. Biophys.* 309 (1994) 77–80.
- [22] A. Nadler, C. Koch, F. Brodhun, J.D. Wehland, K. Tittmann, I. Feussner, U. Diederichsen, Influence of substrate dideuteration on the reaction of the bifunctional heme enzyme psi factor producing oxygenase A (PpoA), *Chembiochem* 12 (2011) 728–737.
- [23] D.A. Pratt, J.H. Mills, N.A. Porter, Theoretical calculations of carbon–oxygen bond dissociation enthalpies of peroxy radicals formed in the autoxidation of lipids, *J. Am. Chem. Soc.* 125 (2003) 5801–5810.
- [24] E.H. Oliw, F. Jermerén, I. Hoffmann, M. Sahlin, U. Garscha, Manganese lipoxygenase oxidizes bis-allylic hydroperoxides and octadecenoic acids by different mechanisms, *Biochim. Biophys. Acta* 1811 (2011) 138–147.
- [25] E.H. Oliw, A. Wennman, I. Hoffmann, U. Garscha, M. Hamberg, F. Jermerén, Stereoselective oxidation of regioisomeric octadecenoic acids by fatty acid dioxygenases, *J. Lipid Res.* 52 (2011) 1995–2004.
- [26] M. Hamberg, Stereochemistry of hydrogen removal during oxygenation of linoleic acid by singlet oxygen and synthesis of 11(S)-deuterium-labeled linoleic acid, *Lipids* 46 (2011) 201–206.
- [27] E.H. Oliw, L. Hörnsten, H. Sprecher, Oxygenation of 5,8,11-eicosatrienoic acid by prostaglandin H synthase-2 of ovine placental cotyledons: isolation of 13-hydroxy-5,8,11-eicosatrienoic and 11-hydroxy-5,8,12-eicosatrienoic acids, *J. Chromatogr. B Analyt. Technol. Biomed. Life Sci.* 690 (1997) 332–337.
- [28] T. Caruso, A. Spinella, Cs₂CO₃ promoted coupling reactions for the preparation of skipped diynes, *Tetrahedron* 59 (2003) 7787–7790.
- [29] C.A. Brown, V.K. Ahuja, Catalytic-hydrogenation. 6. Reaction of sodium-borohydride with nickel salts in ethanol solution – P-2 nickel, a highly convenient, new, selective hydrogenation catalyst with great sensitivity to substrate structure, *J. Org. Chem.* 38 (1973) 2226–2230.
- [30] E.J. Corey, G. Schmidt, Useful procedures for the oxidation of alcohols involving pyridinium dichromate in aprotic media, *Tetrahedron Lett.* (1979) 399–402.
- [31] M. Hamberg, Stereochemistry of oxygenation of linoleic acid catalyzed by prostaglandin-endoperoxide H synthase-2, *Arch. Biochem. Biophys.* 349 (1998) 376–380.
- [32] M. Hamberg, Steric analysis of hydroperoxides formed by lipoxygenase oxygenation of linoleic acid, *Anal. Biochem.* 43 (1971) 515–526.
- [33] M.G. Malkowski, E.D. Thuresson, K.M. Lakkides, C.J. Rieke, R. Micielli, W.L. Smith, R.M. Garavito, Structure of eicosapentaenoic and linoleic acids in the cyclooxygenase site of prostaglandin endoperoxide H synthase-1, *J. Biol. Chem.* 276 (2001) 37547–37555.
- [34] M. Hamberg, B. Samuelsson, Stereochemistry in the formation of 9-hydroxy-10,12-octadecadienoic acid and 13-hydroxy-9,11-octadecadienoic acid from linoleic acid by fatty acid cyclooxygenase, *Biochim. Biophys. Acta* 617 (1980) 545–547.
- [35] R.C. Murphy, R.M. Barkley, K. Zemski Berry, J. Hankin, K. Harrison, C. Johnson, J. Krank, A. McAnoy, C. Uhlson, S. Zarini, Electrospray ionization and tandem mass spectrometry of eicosanoids, *Anal. Biochem.* 346 (2005) 1–42.
- [36] M.O. Funk Jr., J.C. Andre, T. Otsuki, Oxygenation of trans polyunsaturated fatty acids by lipoxygenase reveals steric features of the catalytic mechanism, *Biochemistry* 26 (1987) 6880–6884.
- [37] F. Recupero, C. Punta, Free radical functionalization of organic compounds catalyzed by N-hydroxyphthalimide, *Chem. Rev.* 107 (2007) 3800–3842.
- [38] H. Kitaguchi, K. Ohkubo, S. Ogo, S. Fukuzumi, Additivity rule holds in the hydrogen transfer reactivity of unsaturated fatty acids with a peroxy radical: mechanistic insight into lipoxygenase, *Chem. Commun. (Camb)* (2006) 979–981.
- [39] W.B. Campbell, J.R. Falck, J.R. Okita, A.R. Johnson, K.S. Callahan, Synthesis of dihomoprostaglandins from adrenic acid (7,10,13,16-docosatetraenoic acid) by human endothelial cells, *Biochim. Biophys. Acta* 837 (1985) 67–76.
- [40] D. Picot, P.J. Loll, R.M. Garavito, The X-ray crystal structure of the membrane protein prostaglandin H₂ synthase-1, *Nature* 367 (1994) 243–249.
- [41] H.W. Gardner, Soybean lipoxygenase-1 enzymically forms both (9S)- and (13S)-hydroperoxides from linoleic acid by a pH-dependent mechanism, *Biochim. Biophys. Acta* 1001 (1989) 274–281.
- [42] A.R. Brash, C. Schneider, M. Hamberg, Applications of stereospecifically-labeled fatty acids in oxygenase and desaturase biochemistry, *Lipids* 47 (2012) 101–116.
- [43] C.C. Hwang, C.B. Grissom, Unusually large deuterium-isotope effect in soybean lipoxygenase is not caused by a magnetic isotope effect, *J. Am. Chem. Soc.* 116 (1994) 795–796.
- [44] M.R. Defelippis, C.P. Murthy, M. Faraggi, M.H. Klapper, Pulse radiolytic measurement of redox potentials - the tyrosine and tryptophan radicals, *Biochemistry* 28 (1989) 4847–4853.
- [45] M.J. Nelson, Catecholate complexes of ferric soybean lipoxygenase 1, *Biochemistry* 27 (1988) 4273–4278.